GEOMAGNETICALLY INDUCED CURRENTS AND THEIR EFFECT ON POWER SYSTEMS

BY

TREVOR HUTCHINS

THESIS

Submitted in partial fulfillment of the requirements
for the degree of Master of Science in Electrical and Computer Engineering
in the Graduate College of the
University of Illinois at Urbana-Champaign, 2012

Urbana, Illinois

Adviser:

Professor Thomas J. Overbye

ABSTRACT

High-impact, low-frequency (HILF) events pose a threat to power grids around the world. For example, solar storms that generate coronal mass ejections can induce a change in the Earth's magnetic field. Geomagnetically induced current (GIC) then enters the power grid and causes unusual real and reactive power flows, voltage fluctuations, frequency shifts, undesired relay operations, high third-harmonic currents and telemetry and supervisory alarm failures. A storm on the order of 5,000 nT/min could occur in the not too distant future. Once this storm occurs, widespread damage to the power grid of unprecedented proportions is expected to result. Mitigation strategies are required to protect the integrity of the power system. Mechanisms involved in system restoration need to be prioritized, and the effectiveness of existing black-start procedures needs to be assessed. The representation and simulation of GIC can be embedded into power flow software in order to the study of sensitivity and transient stability of the North American bulk power system under a geomagnetic disturbance (GMD). This thesis presents in-depth background on GMDs and how they affect the power grid. The thesis will continue into the modeling and simulation of GMDs and GIC. Lastly, a GMD scenario will be explored and an appropriate mitigation strategy will be explained.

For Mom and Dad

ACKNOWLEDGMENTS

I would like to thank Professor Thomas J. Overbye for his direction in the research and the writing of this thesis. Also, I express my thanks to my colleagues in the university's Power and Energy Systems research group for their technical insight and support.

Lastly, thanks to my friends and family for their love and support, without which this accomplishment would not have been achievable.

TABLE OF CONTENTS

CHAPTER 1

INTRODUCTION

High-impact low-frequency (HILF) events currently pose a threat to the power grids around the world. Two HILF events of popular discussion include high-altitude electromagnetic pulse detonation (HEMP) and geomagnetic disturbances (GMDs) due to space weather. This thesis concentrates on the effect of GMDs on the power grid. The susceptibility of power grids to GMD events is an ever increasing problem. A single event, lasting just a few minutes, has the potential to cripple portions of the power grid for weeks, even years.

The ability to assess the impact of GMDs on a power system is limited. Tools are not widely available for power engineers to make this assessment. The goal of this research is to develop algorithms for better modeling and mitigating the impacts of geomagnetically induced current (GIC) on the power grid. Comparing actual system measurements, including transformer neutral current, direct field measurements, and actual transformer losses, is a crucial part of this research as the algorithms are developed. This research will allow initial planning studies that will help push GMD assessment into the realm of power system planning and operations engineers. Powerful analysis methods such as transient stability analysis and power flow analysis can be taken advantage of by integrating a GMD tool into existing power flow and transient stability analysis

software. This will enable exploration of short term and long term mitigation strategies of GMD scenarios and their impact on the power grid.

CHAPTER 2

BACKGROUND

2.1 Geomagnetic Disturbances

The geomagnetic disturbances of concern are solar storms, or solar flares. Associated with solar flares are coronal mass ejections. The ejection is plasma consisting mainly of protons and neutrons. The Earth's magnetic field captures the charged particles approximately 20-40 hours after a flare occurs [1]. A violent change in the Earth's magnetic field results, over a period of approximately five minutes, from the capture of the energized solar plasma. The Sun goes through 11-year solar cycles, with solar activity increasing as the cycle nears its end; that is, the end of the cycle is more violent than the beginning [2]. The current solar cycle ends in 2012-2013, and the number of storms per year has also been increasing [2].

The scale used to categorize the intensity of geomagnetic storms is the K-index, or Kp-index. The K-index is a real-time estimate of the Kp-index, which is released only twice per month by the German GeoForschungsZentrum. The K-index considers a minute by minute, three hour window of maximum horizontal component fluctuations of the Earth's magnetic field, measured in nT [3]. The Kp-index is calculated by taking a weighted average of K-indices from a network

of geomagnetic observatories around the world. The index is severely outdated, created in 1932 [4]. The index is a nonlinear mapping of the horizontal component of the Earth's magnetic field. Since most of these magnetometer readings are captured terrestrially, the readings will vary depending on the observatory latitude. Each observatory has a conversion table to convert the magnetometer readings to the appropriate K-index of that area. The index ranges from zero to nine, zero being the minimal GMD.

The K-index suffers from a few key insufficiencies that could be mitigated by using new measurement equipment and techniques. The current scale's bandwidth is too small, and the accuracy of the measurements could be improved with new technology. If an extended K-index scale existed, power system operators could be alerted more accurately. GMDs are measured in nT/min. At the Boulder Geomagnetic Observatory in Colorado, any storm greater than 500 nT/min is classified as a Kp level 9 storm. The effects of a 500 nT/min storm and a 2400 nT/min storm can be very different, the latter, obviously, being significantly more devastating. Currently, several utilities are sent GMD warnings from the National Oceanic and Atmospheric Administration (NOAA) when a potentially dangerous event is detected. According to NOAA, power systems can be perturbed by a storm with a Kp level of 5 or greater [3]. On average, 2600 storms of Kp level 5 or greater happen during the 11-year solar cycle, four of

these being level 9 events [3]. As we will discuss later, in the last 100 years, storms have been recorded over a range of 500 nT/min to 5000 nT/min.

The footprint of a GMD, which traces back to the Sun, can vary drastically. Parameters such as duration, size, direction and polarity, to name a few, of a solar flare all contribute to the final GMD footprint. Contouring the magnitude of the Earth's magnetic field fluxuation provides a visual understanding of the storm's impacted area. Figure 1 shows the footprint from the 1989 Québec storm, with a magnitude of 500 nT/min. Figure 2 shows the footprint of a famous 1921 storm, with a magnitude of 5000 nT/min. The storms are most intense in the center and drop off nonlinearly in a radial fashion. The effects of these specific storms on electrical systems are discussed in Chapter 4.

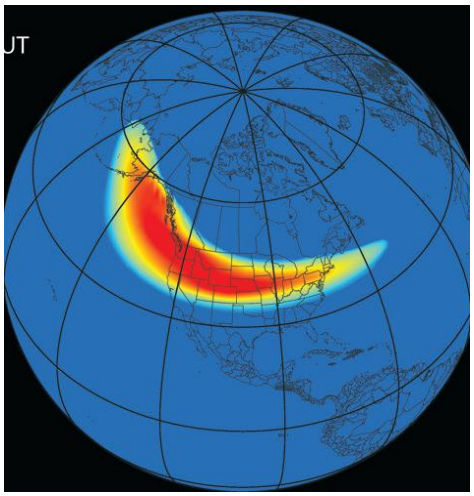

Figure 1. 1989 Quèbec 500 nT/min storm [5]

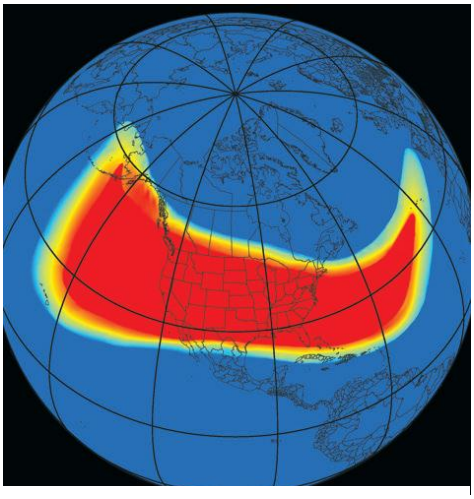

Figure 2. 5000 nT/min storm in 1921 [5]

Figures 1 and 2 display contours of the two different storm magnitudes. These are 'snapshots' during two different storms.

Analogous to a rainstorm, the storm's shape and orientation will be constantly changing throughout the disturbance. Figure 3 shows the changing magnitude of the 1989 Québec storm over 48 hours.

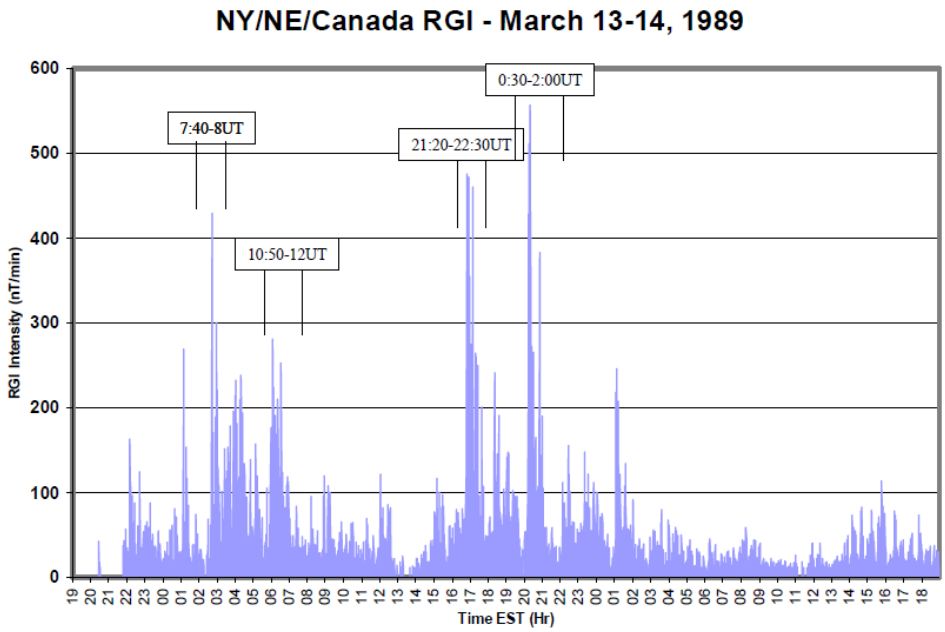

Graph taken from page 48 of [6]

Figure 3. 1989 Québec storm magnitude 48 hour profile

The storm's polarity and orientation will change throughout a GMD. This change is realized as a changing magnetic field density vector field. The magnitude of this vector field at specific time intervals is what characterizes a "storm profile." As the magnetic changes over time, different storm profiles will result.

2.2 Geomagnetically Induced Current

Through Faraday's law of induction, a changing magnetic field density through a defined area, or a changing flux, results in an induced EMF. In this case, the resulting EMF is given by a geomagnetic storm interacting with the Earth's magnetic field over an incremental area, inducing geoelectric fields at the Earth's surface and in the ground. The geoelectric fields drive quasi-dc currents in the ground through high voltage transmission lines, railway equipment, communication cables, and pipeline networks. The frequency of the current is significantly less than the frequency of the electrical grid, so it is said to be quasi-dc. This current is more commonly known as geomagnetically induced current, or GIC. The modeling of GIC is discussed in Chapter 5.

GIC is induced into the power grid when a geomagnetic storm interacts with the Earth's magnetic field. This ionospheric interaction has the ability to perturb the auroral electrojets that circulate the Earth's magnetic poles. These circulating electric currents, electrojets, leave their auroral oval when perturbed. The electrojets are extended at increased strength into the lower latitudes, imposing a geoelectric field, as mentioned before. The accumulated voltage difference between two low-impedance ground points in the power grid yields a current high enough to produce documented damage and power system instability to power grids [7].

The easiest point of entry for GICs into the electric grid is through the grounded neutral wire of wye connected power transformers. These wires are physically grounded in the Earth. These low resistivity wires are the path of least resistance for GIC, when compared to the soil. The high voltage neutral connections are an even easier entry for GIC since their resistivity is less than that of the lower voltage transmission lines. Coincidentally, the higher voltage transformers are damaged easier by excess current flow. The transformers' combination of most at risk and most easily damaged is not ideal for the power grid.

CHAPTER 3

EFFECTS OF GEOMAGNETICALLY INDUCED CURRENTS ON POWER SYSTEMS

3.1 High Voltage Power Transformers

Power transformers, static var compensators (SVCs), and switched capacitor banks are known to suffer from the effects of GIC [1]. Present day power transformers have been optimized to only require a few amps of ac exciting current. The exciting current generates the flux required for the voltage transformation. The amount of flux generated is closely related to the core material which, in the case of the power transformers of interest here, is steel. The steel core's performance is non-linear, as seen in the voltage-current characteristics plot in Figure 4 [7].

Reprinted with permission from T. Hutchins, "The effect of geomagnetic disturbances on the electric grid and appropriate mitigation strategies," in *Proceedings of the North American Power Symposium*, Boston, MA, 2011 [1].

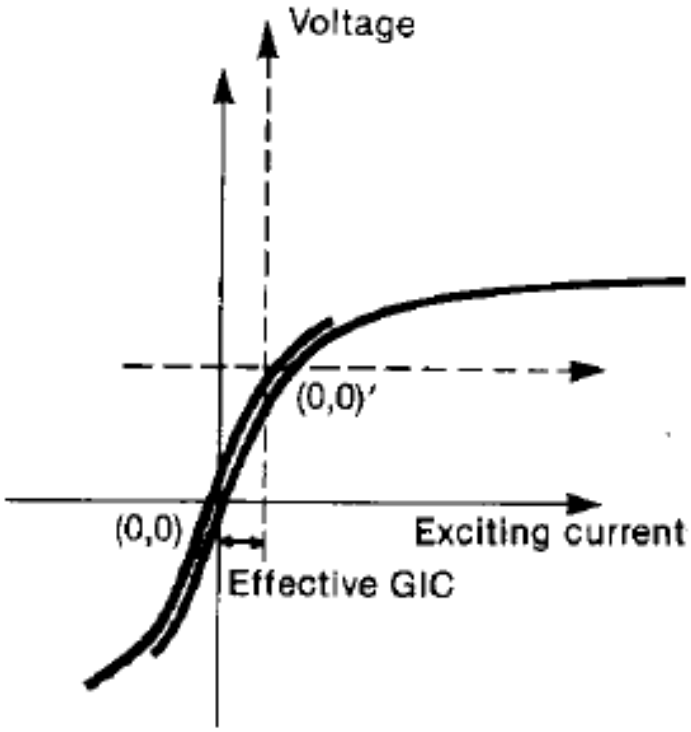

Graph taken from [7]

Figure 4. Steel core performance characteristics of a power transformer

The transformer's core is designed so that the transformer operates only in the linear region. However, under the distress of GIC, the transformer's operating point can be shifted into the nonlinear/saturation region. At the voltage peaks, saturation is seen in the transformer's voltage-current characteristics. As the magnitude of the voltage increases past the linear region, as seen in Figure 4, the voltage begins to saturate. With GICs entering the transformers, the exciting current increases significantly. Positive GIC flow into the transformer severely saturates the positive cycle of the ac exciting current. Field tests from a 600 MVA

transformer, with 75 A of GIC entering the neutral connection, show an exciting current of approximately 300 A, as seen in Figure 5 [7].

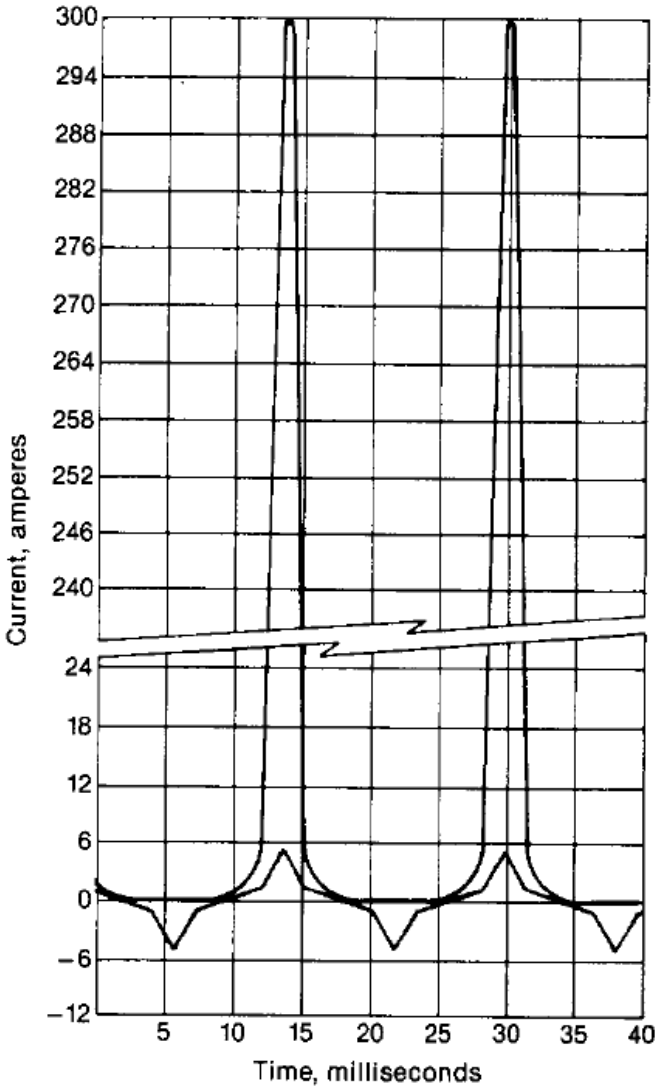

Graph taken from [7]

Figure 5. Half cycle saturation in a 600 MVA transformer with 75 A of GIC flow

The waveform peaking at about 6 A represents a typical excitation current for the transformer. The current, after GIC has been introduced into the transformer, increased asymmetrically to nearly 300A. The operating point of the transformer is no longer in the linear region and it has been pushed far into the positive saturation region. The core is saturated and the flux begins to leak and couple to everything within reach, compromising the transformer's physical and electrical integrity. According to spectrum analysis, the asymmetric exciting current contains several even and odd harmonics [7]. These harmonics are capable of improperly triggering the power line's relays, which is harmful for switched capacitor banks and static var compensators [8]. The distorted excitation current produces severe reactive power losses in the 600 MVA transformer, which suffers a reactive power loss of 50 Mvar with the excitation current of Figure 5 [7]. This translates into a voltage drop in the system that is of serious concern.

Design of a transformer immune to GIC effects has been considered, but the design is cumbersome and the transformer's core size is impractical [7]. Discussed later, a few issues arise when modeling these transformers in a GIC study. Key parameters of the transformer and substation grounding are needed to perform the most accurate GIC calculation, and these parameters are not always readily available. Educated guesses are made in order to provide an approximated GIC calculation, discussed in Chapter 5. In the future, these calculations can be validated with real field measurements. Utilities are currently interested in

installing GIC monitoring devices on key points in their systems. Once these devices have been installed, the calculations can be compared with magnetometer and GIC sensor readings.

3.2 Static Var Compensators and Switched Capacitor Banks

GIC has a significant effect on high voltage transmission lines as well as power transformers. By observing the transmission line equivalent π circuit, as the load increases, the reactive power consumed by the line increases with the square of the line's current [9]. These long lines require support devices such as static var compensators (SVCs) and capacitor banks in an effort to keep the line at the rated voltage. With GIC present, the system is overloaded with reactive power. The voltage of the line drops, and the capacitor banks are switched into the system, as an effort to boost the voltage back to the rated value. The capacitor banks are charged and discharged by the power lines they are connected to through a system of breakers and relays. As mentioned before, the transformer generates unusual even and odd harmonics under GIC conditions [10]. These harmonics are capable of improperly triggering the relays, which results in the improper operation of the system's breakers controlling the SVCs and capacitor banks [10]. During a GMD event, the capacitor banks and SVCs are unreliable and are likely to be destroyed from overcharging [10]. Without devices in the system to help recover from a

voltage drop, the voltage may continue to drop, resulting in the collapse of transmission lines, limiting the power transfer capabilities of the system. A domino effect of power outages can result from this large power loss, initiated by a GMD event [7].

CHAPTER 4

LEARNING FROM THE HISTORY OF GEOMAGNETIC DISTURBANCES

4.1 Hydro Québec System Collapse of 1989

On March 13-14 of 1989, the Earth experienced a geomagnetic storm with a magnitude of 500 nT/min. This storm resulted in the collapse of the Québec Interconnection, and ultimately the entire Québec grid, which collapsed in 25 seconds. The seven static var compensators online tripped, resulting in voltage drop of 0.2 p.u. Through loss of synchronism, the five lines to Montréal tripped, and the entire network separated [4]. The power outage did not extend beyond the Québec Interconnection to the rest of North America. However, power system anomalies were recorded around the globe during the next 24 hour period, including permanent damage to a transformer in New Jersey [4].

In nine hours, 83% of the people affected by the storm in Québec had power restored. In total, 21,500 MW of load and generation were lost [4]. One generator step-up transformer was damaged from overheating due to GICs. If several of these key transformers are damaged, long term outages would be expected. The lead time of a high voltage step-up transformer is 12-24 months [4].

In 1921, a geomagnetic disturbance of approximately 5000 nT/min, ten times the magnitude of the 1989 storm, is believed to have occurred [7]. A storm of this magnitude today would cause widespread damage to the electric grid of unprecedented proportions.

There is some debate about how much a GMD event affects the transformers. Utilities have begun to consider the strategic installation of GIC measurement devices. These devices, coupled with Earth's magnetic field variation data, and reactive power consumption of the transformer, will allow for model validation and improvement. These measurements will also help settle the debate on how severely the transformers are impacted by a GMD event. Understanding how and why the Québec grid collapsed is important when considering GIC mitigation strategies, discussed in Chapter 6.

4.2 Financial Burden of a Geomagnetic Disturbance

The cost of protecting the high voltage transformers in the grid is non-trivial. The preferred method of protection is a topic of debate. The North American Electric Reliability Corporation believes the quickest, and most cost effective, way to protect the transformers is by adding a blocking capacitor or a switchable resistor to the neutral connection of the wye-connected transformers [4], [8]. This research is focused on the system impacts of these devices, not on

the devices themselves. There are several thousand high voltage transformers in the United States electric grid [11]. After cost-benefit analysis, the Electromagnetic Pulse Committee believes that switchable ground resistors are the best option to limit the GIC flow in transformers. The committee estimates the cost of the resistors to be between $75 million and $150 million [11], not including the cost of labor, the sensors used to detect the GIC, or the breakers used to switch in the ground resistors. Since the labor is to be scheduled at the same time of existing maintenance, the cost is substantially reduced from new maintenance orders. In total, the end cost of the units protected is $250 million to $500 million [11]. If a storm similar to the famous 1921 storm, approximately 5000 nT/min, occurs in the near future, the National Academy of Sciences (NACS) estimates a total of 350 high voltage power transformers will be permanently damaged, resulting in a four to ten year recovery period [12]. The transformers are not manufactured in the United States, and this country does not have a sizeable inventory of the high voltage transformers. The transformers currently have a lead time of approximately 12 to 24 months [4]. Due to the physical size of the transformers, they must be brought to the installation location by rail. Many of the railroads used in the past are out of service or no longer exist [4]. During the four to ten year recovery period, 130 million people will be affected in the United States by power disruption [4]. Financially, this has the potential to be the biggest natural disaster the United States has ever faced, with

an estimated loss of $1 to $2 trillion. To put things into perspective, the August 14, 2003, Northeast blackout cost the country between $4 and $10 billion [12].

CHAPTER 5

MODELING GEOMAGNETICALLY INDUCED CURRENT

As mentioned before, the modeling of GIC begins with the interaction between the Earth's atmosphere and the charged particles emitted by the Sun. This interaction results in an induced geoelectric field, an electric field induced at Earth's surface. This geoelectric field then drives GIC through the power grid.

5.1 Geoelectric Field Model

There are several different methods for modeling the interaction between the Sun and the Earth's magnetic field; two methods are described in [13] and [14]. As a starting point for this research, a crude model is used to develop the approximated base geoelectric field. The geoelectric field resulting from the model does not need to perfectly map the interaction of a geomagnetic disturbance. Rather, the modeling of the interaction needs to be accurate enough to produce reasonable, trending geoelectric fields, judged by historical data. The focus of this research is to translate reasonable geoelectric fields into GIC and then understand how that GIC affects a given system.

Reprinted with permission from T. Hutchins, "Power flow studies in the presence of geomagnetically induced currents," in *Proceedings of the Power and Energy Conference at Illinois*, Urbana, Illinois, 2012 [21].

The disturbance causes the Earth's magnetic field to violently change. A non-uniform geomagnetic storm profile, characterized by the rate of change of the magnetic field density vector, B, in units of nT/min, serves as an input to the model. The user has the ability to define the magnitude and direction of the storm. The magnetic field density data used as an input is data that has been recorded terrestrially by magnetometers placed in substations. Not only will the model produce the induced geoelectric field, it will also calculate the accumulated voltage between user-defined geographic coordinates, which are usually the start and end points of transmission lines

The model approximates the interaction between the Sun and the Earth's magnetic field by use of Faraday's law,

$$\int \frac{\partial \mathbf{B}}{\partial t} \cdot d\mathbf{A} = \frac{\partial \boldsymbol{\phi}_{\boldsymbol{B}}}{\partial t} = \varepsilon. \quad (1)$$

The majority of interaction between the Earth's magnetic field and the geomagnetic disturbance is assumed to happen 250 km above the Earth's surface. Using a differential integration length of 1 km, the induced geoelectric field is found by integrating the rate of change of the magnetic field density vector over the differential area, from a user-defined reference point, to a user-defined end point. Due to the Earth's varying ground conductivity, the induced electric field depends on the point of interest. Also, since the storm's magnetic field is not a

uniform field, but rather changing in direction and/or magnitude, different points on the Earth could experience different induced geoelectric fields.

Ground conductivity models, shown in Figure 6, are an important part of precisely mapping the geomagnetic disturbance to a geoelectric field. However, general operation and planning studies can be performed without the inclusion of a ground conductivity model. Uniform fields are a good starting point when studying grid operation under a GMD event. Ground conductivity models become more important when studying systems that span a large geographic region, such as interconnects. The ground conductivity varies significantly across North America, and depending on the ground type, the induced GIC can be significantly impacted. The model illustrated is based on the model in [6]. Layered conductivity profiles contribute to this two-dimensional model. Due to the low-frequency nature of electromagnetic disturbances, ground conductivities of appropriate depths should be considered. Most importantly, the ground conductivity model is better developed by using actual measurements of geoelectric fields and the corresponding GIC at the areas of interest [6]. To illustrate how the ground conductivity changes across America, an example ground conductivity model is shown below in Figure 6, with the different colors representing different ground types in the United States.

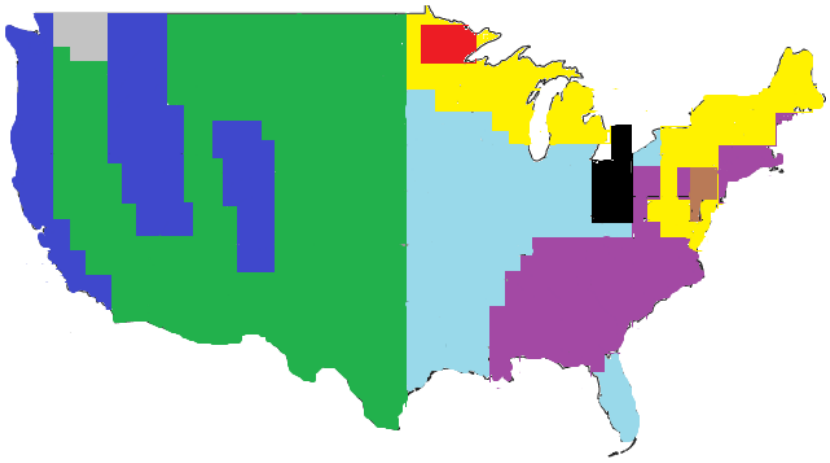

Figure 6. Ground conductivity model of the U.S.A.

Research efforts are under way to further develop the example model and to begin incorporating it in with GIC studies to more precisely model GIC.

5.2 Voltage Source Calculation and Uniform Field Validation

5.2.1 Voltage Source Calculation

After the geoelectric field has been calculated for the areas of interest, the voltage accumulation between the geographical locations must be calculated. The voltage is seen as a voltage source in series with each line [15], but in the end, it is modeled as a Norton equivalent. Modeling the voltage source as its Norton equivalent allows for current injection integration into power flow and transient stability simulation software. The voltage source is calculated based on the geographical coordinates of the system's transmission lines and the geoelectric

field generated by the model. The distance between the start and end points of each transmission line is multiplied by the areas geoelectric field to determine the voltage difference between the end points. As mentioned before, the model in this algorithm uses a quasi-finite element method with a resolution of approximately 0.5 x 0.5 degrees. The voltage is calculated according to Equation (2).

$$V_{dc} = \oint \mathbf{E} \cdot d\boldsymbol{l} \tag{2}$$

In words, the induced voltage is calculated by integrating the projected electric field along a closed path, for example, transmission lines between grounded wye transformers. The dot product multiplication is very important, since this is how the angle/orientation of the storm is accounted for. How the modeled voltage is implemented is discussed in section 6.3.

5.2.2 Uniform Field Validation

The previous algorithms were implemented in MATLAB. To begin the validation of the model's voltage source calculation, a uniform northward geoelectric field and an eastward geoelectric field are applied at separate times, representing two different storms, as seen in Equations (3) and (4).

$$\boldsymbol{E} = 1.0\boldsymbol{x} + 0.0\boldsymbol{y}\ V/km \tag{3}$$

$$\boldsymbol{E} = 0.0\boldsymbol{x} + 1.0\boldsymbol{y}\ V/km \tag{4}$$

Equation (3) is a uniform northward field, vectorially South to North, with a constant magnitude of 1.0 V/km. Equation (4) is a uniform eastward field,

vectorially West to East, also with a constant magnitude of 1.0 V/km. Forcing the geoelectric field to 1.0 V/km allows for easy validation. Since the magnitude is 1.0 V/km in both storms, the accumulated voltage will be equal to the distance in the South-North direction for Equation (3) and the West-East direction for Equation (4). The "actual" voltage source values were found by using the haversine formula to calculate the great-circle distance between two points. Since the geoelectric field is 1 V/km, the "actual" voltage source is equal to the "actual" distance calculated. Fictitious buses were assigned to the geographical coordinates listed in Table 1. It is assumed that each bus listed has a closed loop path between the 'from' bus and 'to' bus via transmission lines with grounded wye connections on either end.

Table 1. Geographical coordinates of the system's buses

Line	From Bus (degrees)	To Bus (degrees)
1	(30, -85)	(33, -86)
2	(31, -88)	(35, -83)
3	(30, -85)	(35, -83)
4	(34, -79)	(34, -82)
5	(36, -80)	(35, 80)

The results of the algorithm are compared to the "actual", or haversine distance calculation, voltage source values in Table 2. The percent error is very small. For this brief uniform field validation, the calculated voltage sources are

nearly identical to the actual, or exact, voltage calculations, shown in Table 2. The error that does exist is attributed to the use of the Mercator projection. For preliminary studies, this estimate in the Mercator projection was sufficient; however, as the algorithms were worked into power flow simulation software, a more accurate distance calculator was required.

Table 2. Uniform field validation results

Line	Northward Vsource Actual (V)	Northward Vsource Model (V)	Eastward Vsource Acutal (V)	Eastward Vsource Model (V)	Northward Vsource % Error (%)	Eastward Vsource % Error (%)
1	333	336	-90	-91.67	0.90	1.85
2	444	448	449	458.34	0.90	2.08
3	556	560	180	183.33	0.72	1.85
4	0	0	-270	-275.00	0.00	1.85
5	-111	-112	0	0.00	0.90	0.00

The algorithms have been further developed and directly implemented into PowerWorld Simulator in accordance with [16]. The calculation now accounts for the non-spherical shape of the Earth and uses the WGS84 Earth model, which is used in the GPS system [16]. More accurate distance calculations allow for higher accuracy in the induced voltage source calculations.

5.3 Modeling Geomagnetically Induced Currents

Caution must be taken when considering the modeling of GIC. For uniform geoelectric fields, it is acceptable to model the induced voltage as voltage sources in the ground connection of the transformers, as an Earth surface potential [15]. A uniform electric field is "conservative," meaning the integration of the electric field is not dependent on the chosen path; thus, the integral around the closed loop is zero [15]. The integral around a closed loop is no longer zero when realistic electric fields are considered, due to the vector function component of a realistic field [15]. It has been shown that modeling realistic geoelectric fields with the ground source method is incorrect [15]. The fields should be modeled as voltage sources in the transmission lines, in accordance with Equation (2).

When performing the line integration of the electric field, it is very important to consider the direction of the field. For example, if a transmission line is perpendicular to the direction of the geoelectric field, there will be no induced voltage in that line, since the dot product, seen in Equation (2), will return a value of zero. Depending on the topology of the power system, it could be extremely vulnerable to certain orientations of geoelectric fields, and unaffected by other orientations. Consider the system below in Figure 7.

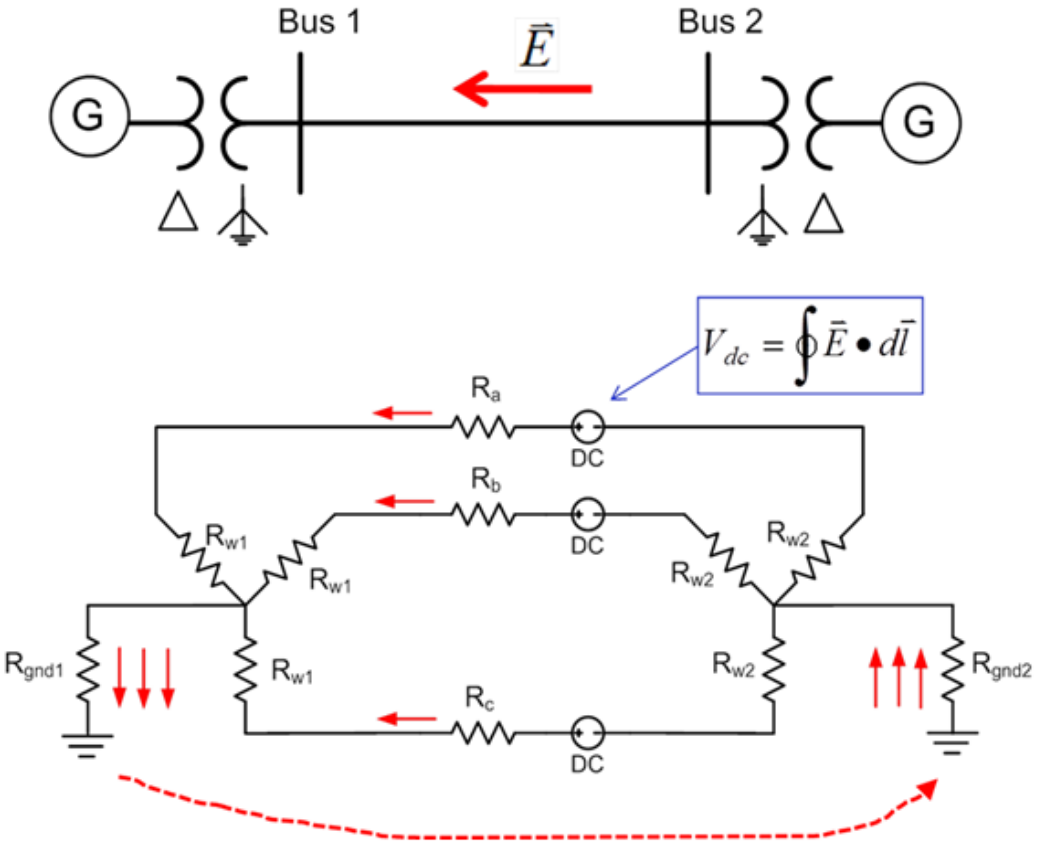

Figure 7. GIC flow and voltage source placement

Notice the flow of GIC in the power system shown in Figure 7. The GIC enters and exits through the grounded neutral of the wye connected transformer. With the combined knowledge of the induced transmission line voltage sources and a power system's substation grounding and transformers design, the GIC can be calculated. Since GIC is low frequency, below 1 Hz, the system's reactances can be ignored when calculating the GIC [8]. The GIC flows can be determined from solving the linear dc network:

$$I = G_{bus(augmented)}V \tag{5}$$

The augmented admittance matrix seen in Equation (5) is altered to include substation neutral impedances. A sample calculation of a fictitious system is given in the following section.

5.4 Sample GIC Calculation

To demonstrate the calculation of GIC flow in detail, consider the four bus power system in Figure 8. The system has been exposed to a left-right geoelectric field of 1.5 V/km. The length of the transmission line between buses one and three is 100 km.

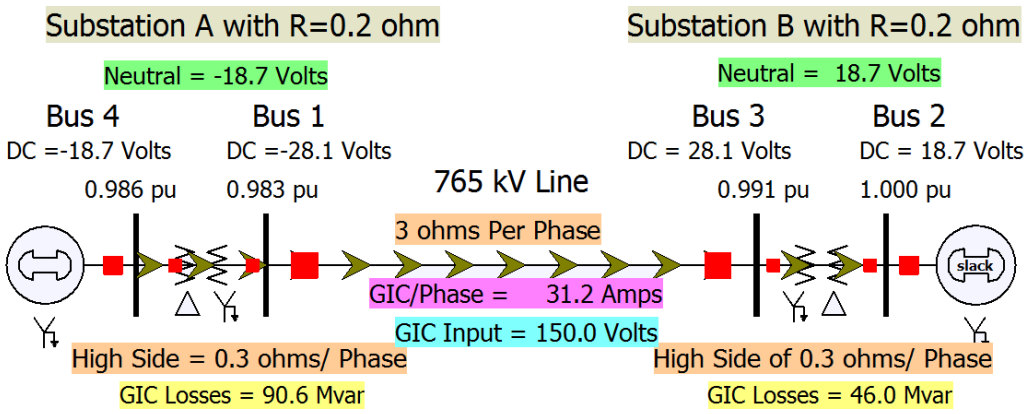

Figure 8. Oneline diagram of an example four bus power system

This system has two generators, two high voltage generator step-up transformers that are grounded wye, and a high voltage transmission line connecting the two transformers. The integration of the electric field has already

been performed and an inline voltage source value of 150.0 V results. The 150 V serves as an input to this GIC model. The brown arrows represent the direction and magnitude of the calculated GIC. Explicitly noted in the oneline diagram are the substation grounding resistances, transformer winding resistances, and the resistance of the transmission line. All of these values are required to accurately calculate the GIC. The GIC is calculated by first augmenting the system to include the substation ground buses and then performing nodal analysis. The system is augmented according to Figure 9.

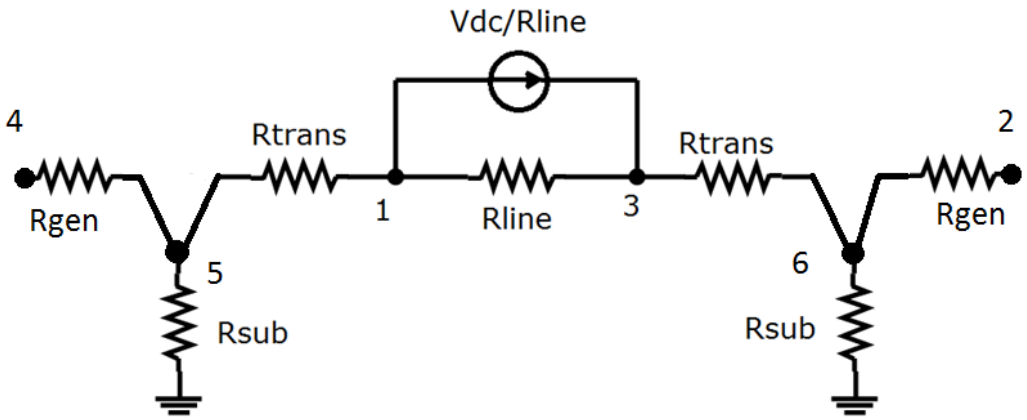

Figure 9. Augmented dc network

The first thing to notice is that the diagram now includes buses five and six, with open ends on nodes two and four. The existence of the delta connection between buses 1 and 4, and buses 2 and 3, prevents the GIC from flowing through generators. The inline voltage source has been converted to its Norton equivalent, and will serve as a current injection in the Nodal analysis. Also, consistency in

single phase, or three phase value of resistance is of high importance. As mentioned before, the GIC enters and exits through the grounded transformers, but it splits evenly among the three phases of the transmission line. In the following calculations, three phase resistance values are used. Symbolically, Equation (5) evaluates to

$$\begin{bmatrix} G_{11} & 0 & G_{13} & 0 & G_{15} & 0 \\ 0 & G_{22} & 0 & 0 & 0 & G_{26} \\ G_{31} & 0 & G_{33} & 0 & 0 & G_{36} \\ 0 & 0 & 0 & G_{44} & G_{45} & 0 \\ G_{51} & 0 & 0 & G_{54} & G_{55} & 0 \\ 0 & G_{62} & G_{63} & 0 & 0 & G_{66} \end{bmatrix} \begin{bmatrix} V_1 \\ V_2 \\ V_3 \\ V_4 \\ V_5 \\ V_6 \end{bmatrix} = \begin{bmatrix} -V_{dc}/R_{line} \\ 0 \\ V_{dc}/R_{line} \\ 0 \\ 0 \\ 0 \end{bmatrix}. \quad (6)$$

Since the resistance of the generators is not known, a value of 1 is assigned, to prevent the conductance matrix from being singular. It should be clear that this number only assists in the matrix inversion. Since there is no current flow in the branch connecting nodes four and five, the assigned resistance does not matter, as long as the chosen value does not make the matrix ill-conditioned. Substituting the values into Equation (6) and solving, the following dc voltages result:

$$\begin{bmatrix} 11 & 0 & -1 & 0 & -10 & 0 \\ 0 & 1 & 0 & 0 & 0 & -1 \\ -1 & 0 & 11 & 0 & 0 & -10 \\ 0 & 0 & 0 & 1 & -1 & 0 \\ -10 & 0 & 0 & -1 & 16 & 0 \\ 0 & -1 & -10 & 0 & 0 & 16 \end{bmatrix}^{-1} \begin{bmatrix} -150 \\ 0 \\ 150 \\ 0 \\ 0 \\ 0 \end{bmatrix} = \begin{bmatrix} V_1 \\ V_2 \\ V_3 \\ V_4 \\ V_5 \\ V_6 \end{bmatrix} = \begin{bmatrix} -28.125 \\ 18.75 \\ 28.125 \\ -18.75 \\ -18.75 \\ 18.75 \end{bmatrix} V. \quad (7)$$

The three-phase GIC flow can now be calculated by Ohm's law, in accordance with the system topology,

$$GIC_{3\varphi} = G_{sub} V_5 = 5 * -18.75 = -93.75\ A. \quad (8)$$

The GIC in each phase of the transmission line can be found by dividing the three phase GIC by three, to achieve 31.25 A.

5.5 Reactive Power Demand of a GIC Saturated Transformer

Figure 8 also shows the amount of GIC losses, or Mvar demand, of the transformer, determined from the GIC calculation. Here, the Mvar demand of the transformer due to the GIC is modeled with a linear mapping of the GIC, varying with a voltage squared term. Research is under way to determine the best way to model the Mvar losses. Currently, the research is leaning towards a constant current model, since the Mvar loss varies linearly with current. It is understood that different transformer types will demand reactive power differently under GIC conditions [17] and [18]. Depending on the transformer's core design, different coefficients are used to map the Mvar demand due to GIC [18]. These coefficients are regressed from Figure 10.

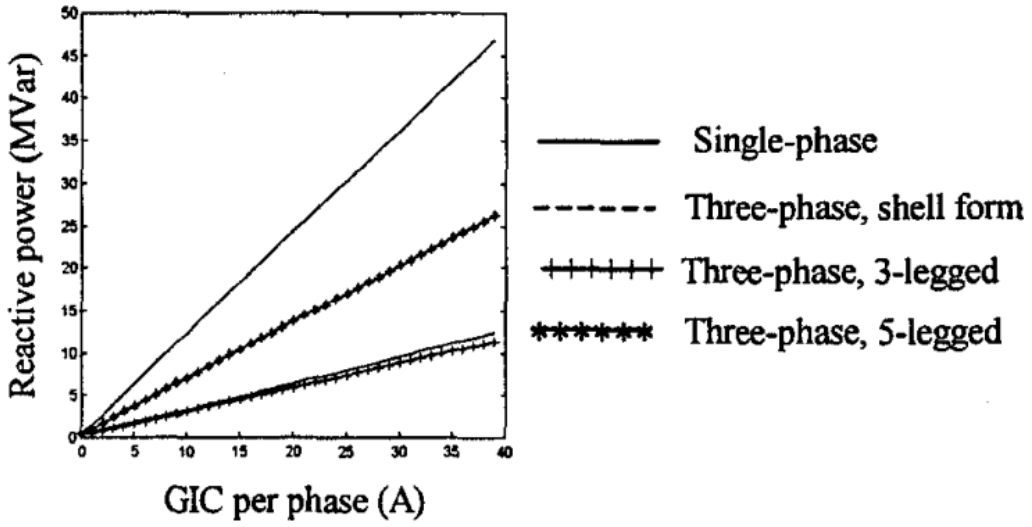

Figure taken from [18]

Figure 10. The variation of the Mvar consumption vs. the input GIC per phase

The harmonics generated by the transformer saturation are not included in the GIC losses. The reactive power demand of the transformer is calculated with only the fundamental component and the exciting current [17], [18]. The calculation is given in [18] by Equation (9) with coefficients listed in Table 3.

$$Q(Mvar) = k_1 * GIC + Q_0 \quad (9)$$

GIC is the total three phase GIC. Q_0 is the reactive power loss due to the exciting current. The coefficient dependent on the core type is k_1, given in Table 3.

Table 3. Coefficients for different core types

Core Design	k_1
Single phase	1.18
Three-phase, shell form	0.33
Three-phase, 3-legged, core form	0.29
Three-phase, 5-legged, core form	0.66

As shown in Equation (9) and Table 3, the Mvar demand can vary significantly depending on the transformer's core type. Also seen in Equation (9), the reactive power demand of the transformer increases with the GIC. The generation of a system must be increased in order to support the demanded reactive power as the GIC increases. The increased current, due to the increased generation, translates into voltage drops across the system as losses are seen in the transmission lines, as experienced by Québec in 1989 [4]. Consider the EPRI 20 bus case with nominal loading of 4700 MW and 1800 Mvar in Figure 11.

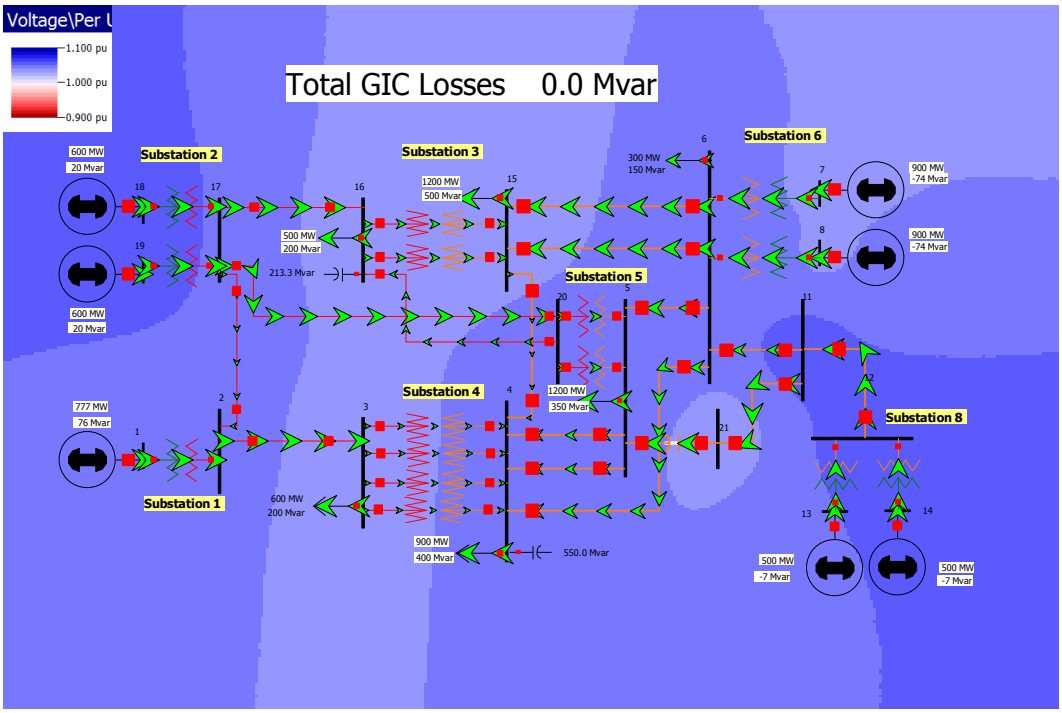

Figure 11. EPRI 20 bus system at 4700 MW and 1800 Mvar loading

The arrows in Figure 11 represent the real power flow in the system. Notice that no GIC has been induced in the system since the "Total GIC Losses" is 0 Mvar. As the GIC is increased, it is expected that the system will begin to experience a voltage collapse, as seen in Figure 12.

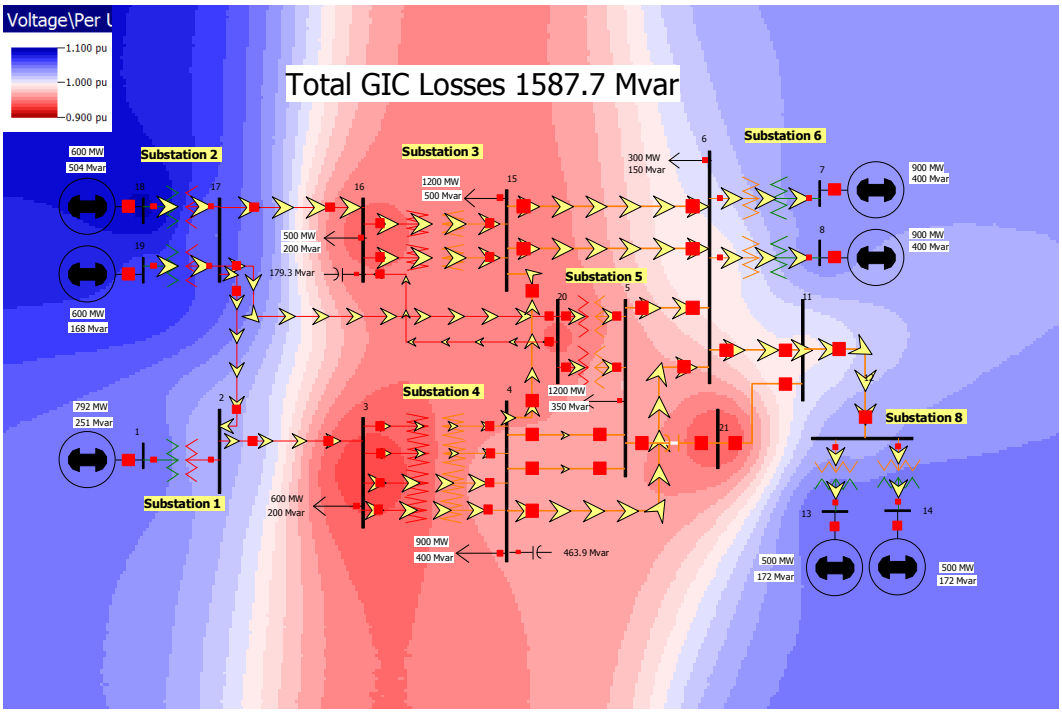

Figure 12. 2.2 V/km East-West geoelectric field on the EPRI 20 bus system

The arrows in Figure 12 represent the GIC flowing in the system. It is important to note that the ac power flow solution and the GIC dc network solution are being calculated simultaneously. This allows for the study of voltage collapse in the presence of GIC. The ability to contour the system's voltage at each bus allows for quick diagnosis of power flow problem areas. This problem is ultimately mitigated by reducing the amount of GIC in the system, which is described in Chapter 6.

CHAPTER 6

MITIGATING THE EFFECTS OF GIC

A blocking device on every grounded wye power system component would prevent GIC from entering the system. However, this is not a viable option. First of all, it is unclear what would happen if the system was ungrounded at the dc level. This could create safety issues and should be studied further. Also, two other major issues with protecting every high voltage transformer in the electric grid from GIC are time and money. In order to protect the high voltage transformers, a standard of protection must first be established across all utilities. Next, the transformers must be retrofitted with the GIC protection device. With the next major geomagnetic storm imminent, the time required in order to protect the transformers is too long. It has been suggested that these devices be installed during existing maintenance periods [11]. This solution makes sense for the long term problem, but the near term threat is still present.

6.1 WSCC Nine Bus – Short Term Case Study

Consider the induced line voltages of Table 4, in reference to the WSCC nine bus power system [19], diagrammed in Figure 13.

Table 4. Line voltage inputs due to a GMD

From Bus	To Bus	Line Vsource (V)
6	4	-75
9	6	-20
2	7	0
9	3	0
7	5	20
4	1	25
5	4	75
8	9	150
7	8	150

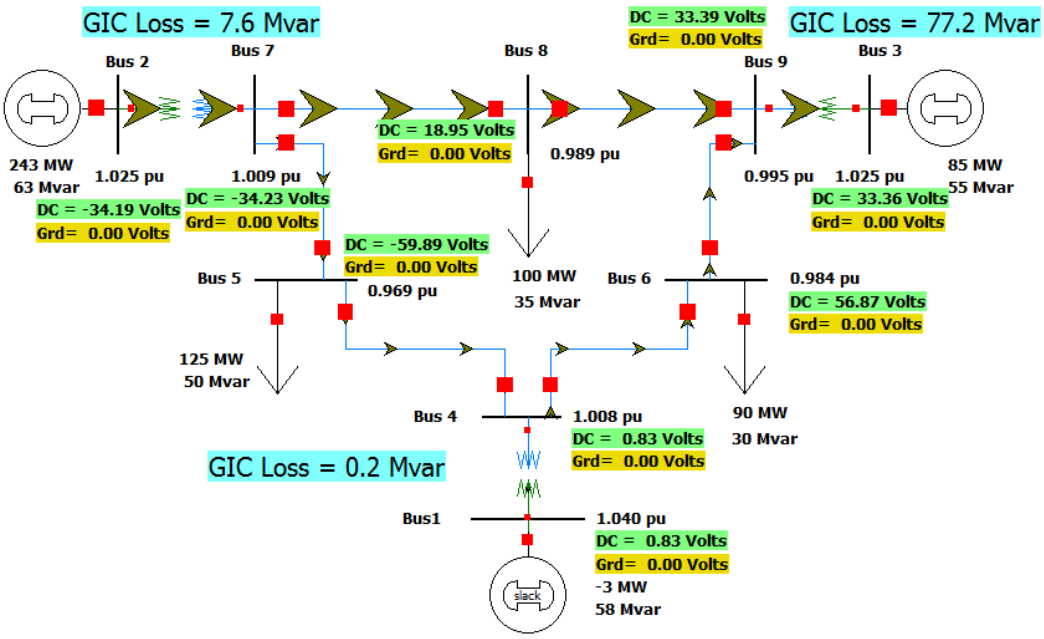

Figure 13. WSCC nine bus power system model under GIC distress

As before, the magnitude and direction of the brown arrows in Figure 13 represent the flow of GIC. The increased Mvar demand on the system, due to GIC, is noted as "GIC Loss." It should be apparent from Table 4 that a geoelectric field of left to right bias was imposed on the system. This can also be deduced from the direction of the GIC arrows. The longest left-to-right transmission corridor, bus 7 to bus 9, experiences the largest GIC. This is expected since the path of integration is the longest and parallel to the geoelectric field. If the geomagnetic disturbance is strong enough, the GIC will be so large that the system can no longer handle the reactive power being demanded. The system will then collapse, resulting in a system wide power outage. The GIC is entering into and exiting from the WSCC nine bus system through the grounded wye-connected neutrals of the transformers. In the long term, a utility would want to study a variety of different storm scenarios to determine where to place a GIC blocking device. The most obvious solution is to have a GIC blocking device, such as [20], installed on the transformer connecting bus 2 to bus 7. This would prevent all GIC from entering the system at that transformer. Although the devices are expensive, they are far less expensive than repairing or replacing a high voltage transformer. At the same time, the expense in both time and money of installing a GIC blocking device on every transformer makes it impractical.

The strategy proposed focuses on the short term scenario, explained below. Consider the scenario of utility X, operating the power system seen in

Figure 13, under the geomagnetic disturbance conditions of Table 4. The utility has no GIC blocking devices installed. Plans to install future devices are irrelevant at the moment because the utility has just received word from the National Oceanic and Atmospheric Administration that a very large geomagnetic disturbance is about to reach Earth. Given some previous knowledge of the storm, the power system operators are told the storm's magnitude and direction. The power system operators then use their knowledge of the system to redistribute power in the system to limit the impact of the geomagnetic disturbance.

If it were possible to open the line between bus 7 and bus 8, the introduction of GIC into the system would be significantly reduced. The wye-connected transformer between bus 2 and bus 7 is no longer required to provide the power to the load at bus 8, and there is no longer a path for the GIC to flow directly between bus 7 and bus 9. The effect of the mitigation strategy is illustrated in Figure 14.

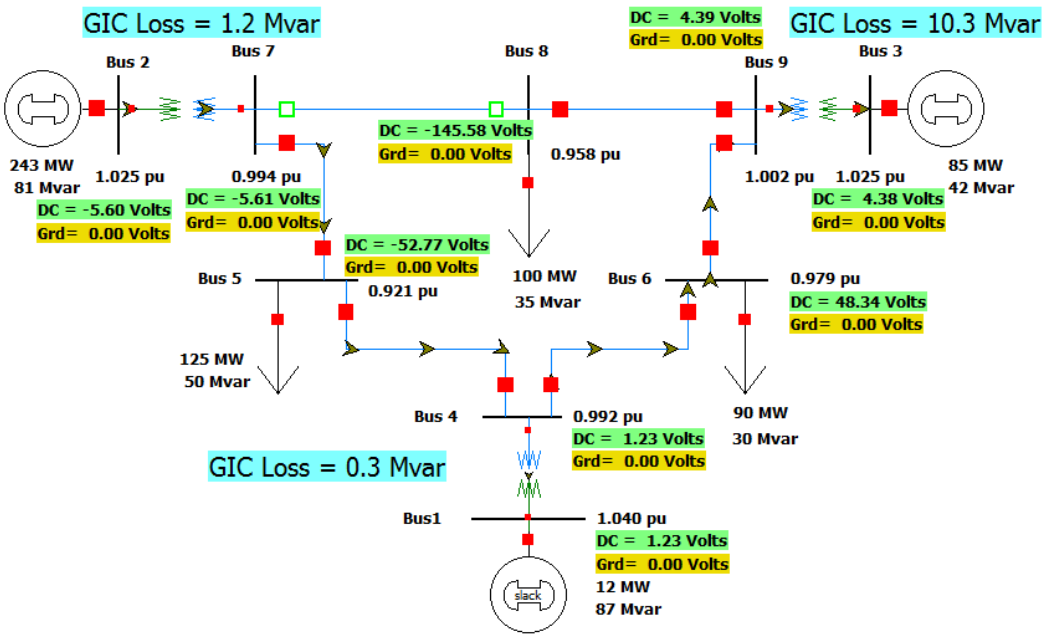

Figure 14. WSCC nine bus under short term mitigation

The generator at bus 1 must increase its generation to account for the change in the power system's topology. The power has been rerouted to the load at bus 8, and is now being supplied in part by the generator at bus 1. It is clear that the system's vulnerability to a left-to-right geomagnetic disturbance is reduced with the outaged line. Power no longer travels as much in the left-to-right direction as it did before. Note the total amount of GIC loss in the system; it went from 85.0 Mvar to 11.8 Mvar, an 86% reduction. Utility X was able to keep all its customers in service and reduce the reactive power demand on the system by cleverly taking a line out of service.

6.2 EPRI 20 Bus – Long Term Case Study

Long term mitigation strategies can be vastly different from short term ones. Here, the long term mitigation problem of interest is where to install GIC blocking devices, and how many are required. When considering long term mitigation strategies, it is important to analyze the system of interest under several different GMD events. The system needs to be resilient to storms inducing geoelectric fields at any angle. As mentioned before, a system may be mostly unaffected by a particularly directed geoelectric field but extremely vulnerable to a geoelectric field oriented in another direction. With this in mind, it would only make since to protect the system from the geoelectric field direction of most impact.

However, it is possible that a power system could be vulnerable to geoelectric fields at a multitude of angles. Simulating the effects of geomagnetic disturbances on a system, while varying the orientation of the geoelectric field, will allow for a comprehensive study of the system's vulnerability. Determining the vulnerability of a system should be the first step in the long term mitigation strategy planning procedure.

Consider the EPRI 20 Bus system in Figure 15, with the substation located as noted in Table 5. The system is subjected to a 5 V/km storm at orientations of 0°, 45°, 90°, and 135°. Northward corresponds to 0° and eastward corresponds to

90°. It is unnecessary to sweep the storm angle a full 360°. A 180° sweep is sufficient since the Mvar demand on the system will be the same if the storm is oriented in the exact opposite direction. The results are in Table 6.

Table 5. EPRI 20 bus substation geographical coordinates

Substation	Latitude (Degrees)	Longitude (Degrees)
1	33.613499	-87.3737
2	34.310437	-86.3658
3	33.955058	-84.6794
4	33.547885	-86.0746
5	32.705087	-84.6634
6	33.377327	-82.6188
7	34.252248	-82.8363
8	34.195574	-81.098

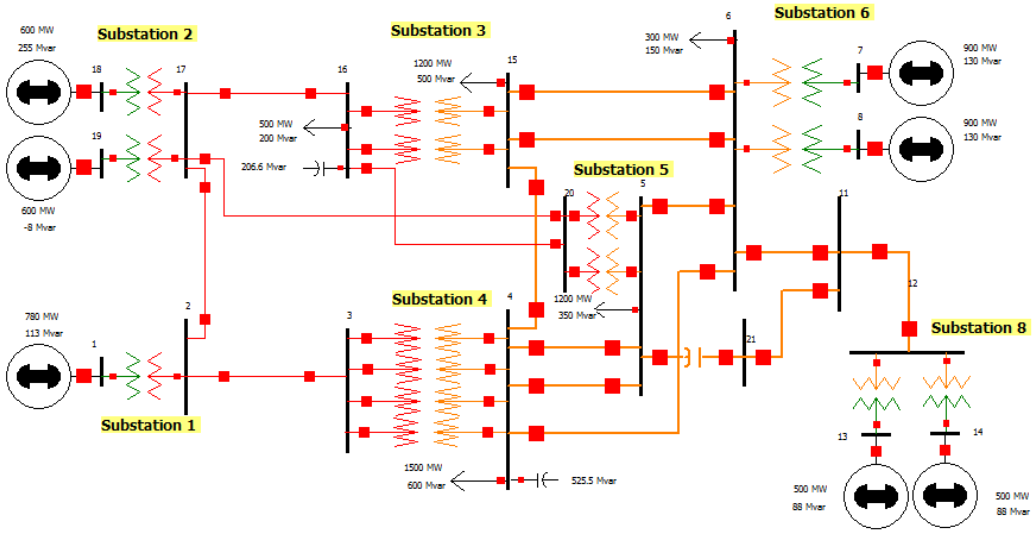

Figure 15. EPRI 20 bus system

Table 6. Mvar demand due to a 5 V/km geoelectric field at different orientations

Transformer		Transformer Mvar Coefficient	GIC Mvar Losses (Mvar)				Totals (Mvar)
From Bus	To Bus		0 degrees	45 degrees	90 degrees	135 degrees	
1	2	0.5	37.1	428.7	569.1	376.2	1411.0
3	4	1	36.0	99.5	176.7	150.5	462.7
3	4	1	36.0	99.5	176.7	150.5	462.7
3	4	1	43.0	122.1	215.6	182.9	563.6
3	4	1	43.0	122.1	215.6	182.9	563.6
20	5	1	720.3	542.8	301.6	475.9	2040.5
20	5	1	720.3	542.8	301.6	475.9	2040.5
6	7	0.5	77.2	310.2	515.8	419.3	1322.4
6	8	0.5	77.2	310.2	515.8	419.3	1322.4
12	13	0.5	82.4	188.2	183.7	71.7	525.9
12	14	0.5	82.4	188.2	183.7	71.7	525.9
16	15	0.7	238.0	83.9	210.9	317.4	850.2
16	15	0.7	238.0	83.9	210.9	317.4	850.2
18	17	0.5	173.0	21.5	142.6	223.2	560.3
19	17	0.5	166.6	20.7	137.3	214.8	539.4
		Totals (Mvar)	2770.5	3163.8	4057.6	4049.3	14041.2

This particular system appears to be susceptible to geoelectric fields in all directions. This can be deduced by observing the total Mvar demand on the system at the bottom of Table 6. With the chosen 45° resolution, this system experiences the largest Mvar demand when the geoelectric field is oriented in the East-West and West-East directions, or 90° and -90°. Depending on the system's

generation capability, available GIC blocking devices, and constraints, the optimal mitigation strategy can be very different.

The total Mvar demand due to each transformer from all the storms is shown in the rightmost column of Table 6. These values can be helpful when determining where to place blocking devices. Placing a blocking device on a transformer prevents GIC from entering/exiting that point. The Mvar demand due to that transformer will be zero after a device is installed. However, it should be noted that the GIC in the system will try to find another path that it can exit, since it can no longer exit the blocked transformer. In some cases, blocking a particular transformer will have no effect on the overall Mvar demand on the system because the GIC will find an alternate path to exit. Consider blocking the two transformers between bus 20 and bus 5, shown in Table 7. The total Mvar demand for each storm was significantly reduced. On average, the demand on the system was reduced by 32% per storm. This 32% reduction could be enough to keep the system from experiencing long term outages.

Table 7. EPRI 20 bus system with blocking devices on the transformers between bus 20 and bus 5

Transformer		Transformer Mvar Coefficient	GIC Mvar Losses (Mvar)				Totals (Mvar)
From Bus	To Bus		0 degrees	45 degrees	90 degrees	135 degrees	
1	2	0.5	110.9	490.1	582.2	333.3	1516.5
3	4	1	16.7	148.5	193.4	124.9	483.5
3	4	1	16.7	148.5	193.4	124.9	483.5
3	4	1	15.2	176.3	234.2	154.8	580.5
3	4	1	15.2	176.3	234.2	154.8	580.5
20	5	1	0.0	0.0	0.0	0.0	0.0
20	5	1	0.0	0.0	0.0	0.0	0.0
6	7	0.5	192.8	208.4	487.5	481.0	1369.8
6	8	0.5	192.8	208.4	487.5	481.0	1369.8
12	13	0.5	72.1	179.1	181.2	77.2	509.5
12	14	0.5	72.1	179.1	181.2	77.2	509.5
16	15	0.7	131.7	60.5	217.2	246.7	656.2
16	15	0.7	131.7	60.5	217.2	246.7	656.2
18	17	0.5	109.2	10.3	123.8	164.7	408.0
19	17	0.5	105.1	10.0	119.2	158.6	392.8
		Totals (Mvar)	1181.9	2056.0	3452.1	2826.0	9516.0

Understanding the redistribution of GIC with added blocking devices is crucial to the future of this research. Placing a blocking device on one of the transformers between bus 20 and bus 5 will not help in any manner, other than physically protecting the transformer. The GIC will redistribute and flow into the parallel transformer. A simple strategy could be to block the transformers that have high Mvar demand coefficients. By blocking the transformers that are the

most physically vulnerable, the GIC will be forced into the transformers that are inherently less susceptible to the problem.

This research will expand into the development of algorithms to optimally reduce the effects of a GMD on a given system. Geomagnetically induced current sensitivity analysis will aid in the development of these algorithms.

CHAPTER 7

POST-DISASTER RESTORATION

As explained in Chapter 6, in the event of a near term geomagnetic disturbance, it is not plausible to protect all the high voltage transformers in the power grid. In the event a storm destroys several high voltage transformers, a proposed transformer bypass method is presented. If several of these transformers are destroyed, it is likely that the system will no longer be operational, and the users will be left powerless. Critical transformers can be bypassed and grid users will once again be receiving power. This is somewhat of a "last resort" method, considering the physical structure of the network will have to be changed. But, it is a viable solution to restoring power to the grid if the high voltage transformers are destroyed. They bypassing of the transformers is explained in this chapter.

7.1 High Voltage Transformer Bypassing

The power system of Figure 16 contains one high voltage generator step-up transformer and one high voltage step-down transformer.

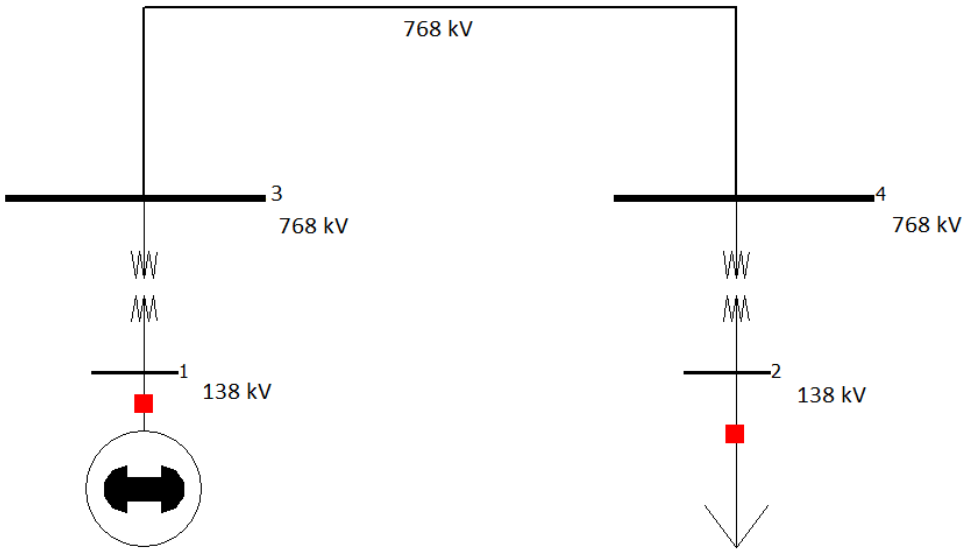

Figure 16. Four-bus high-voltage power system

Each transformer is connected between a bus at 138 kV and a bus at 768 kV. Figure 16 shows the nominal ideal voltages of the transmission system. In order to bypass the transformer, a transmission line is connected in parallel with the transformer. The power flows around the transformer, and now, all transmission lines connected to the transformers terminals are operating at 138 kV, as seen in Figure 17.

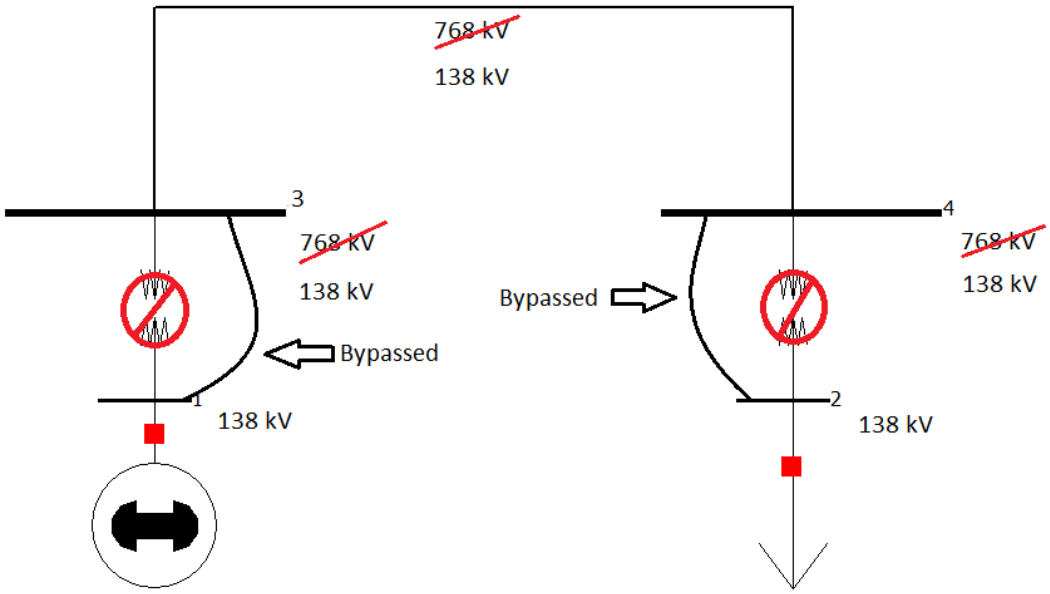

Figure 17. High voltage power system with transformer bypassing

Bypassing the transformers in this manner allows for the use of the original transmission topology. The only downtime the load sees is the time it takes the utility to install the patch transmission line. Figure 17 shows the system's voltages after the transformers have been bypassed with transmission line. Since the transformers are being bypassed, the voltage and current are not transformed. The transmission lines will be operating at the pre-transformed voltage and current. There is concern that the current may be too high for the higher voltage lines; this concern is addressed in a 37 bus case-study in the next section.

7.2 A 37 Bus Case Study

Studying grid operation after many transformers have been destroyed can help utilities. Critical infrastructure analysis can be performed in order to determine the critical high voltage transformers in the grid. In the 37 bus case, there are six high voltage transformers. By inserting contingencies in PowerWorld Simulator, each of the transformers can be disabled. Since there are only six high voltage transformers in this study, it is simple to determine which transformers are crucial to the system. By trial and error, it was determined that as few as two transformers are required to maintain the full integrity of the system. If any two of the transformers were protected, the system suffered no outages. The 37 bus system is seen in Figure 18. This post-scenario study focuses on the event that a geomagnetic storm has occurred, and with no preventative measures in place, all six high voltage transformers in the 37 case system were destroyed. If all six transformers are destroyed, the outside generation has no chance of supplying the system with power, and the system will collapse. To be clear, the GMD event has already happened, and the system is no longer under GIC stress, experiencing Mvar demand. However, the high voltage transformers have been permanently damaged. As explained earlier, the destruction of several high voltage transformers could mean long term outages, lasting even years. In an effort to

restore power to the system quickly, two of the blown transformers were bypassed with transmission line.

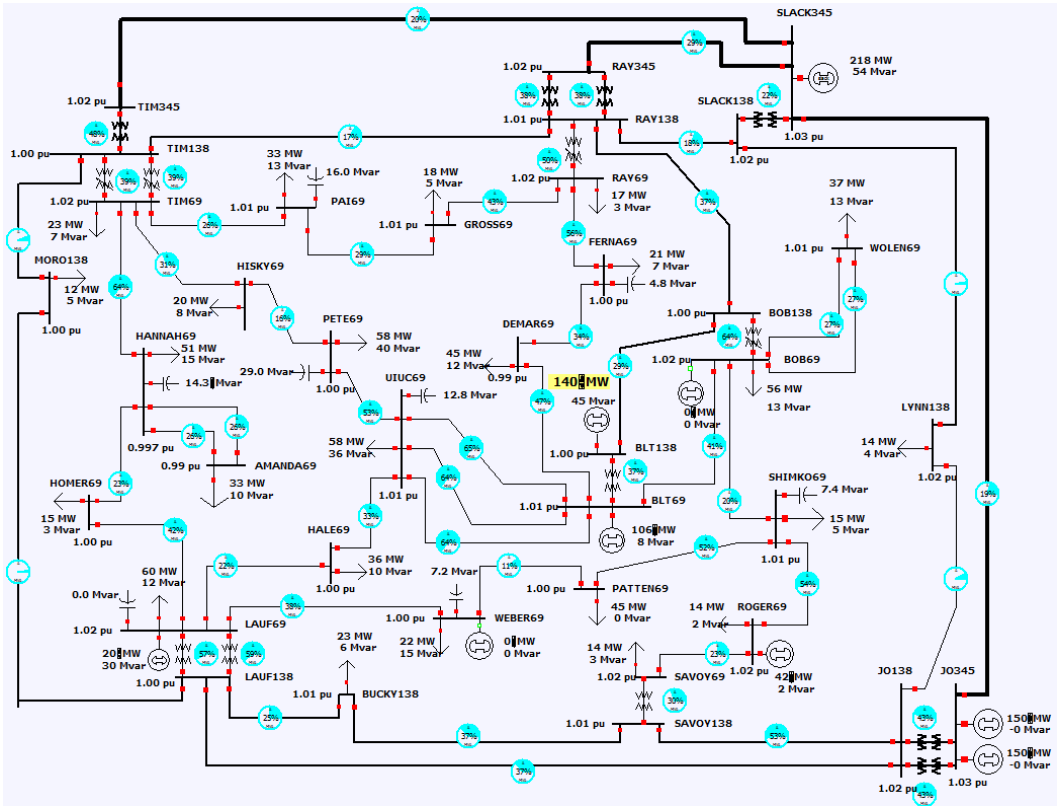

Figure 18. The 37 bus case study topology

In the simulation, the transformers are bypassed by replacing them in the oneline diagram with a transmission line. The impedance of the transmission line is that of the pre-transformed voltage line impedance. The high voltage lines are now operated at a lower voltage so their impedance must be modeled with the impedance of the operated voltage. In reality, the generator step-up transformer would be damaged. Utilities would bypass the transformer with transmission line.

Now, the high voltage line would be operated at the pre-transformed voltage since the transformer was bypassed. It is of notable concern that the current will be higher since the line is operated at lower voltage. The power flow solution, seen in Figure 19, accounts for the higher current by modeling the line impedance as the impedance of the lower voltage lines.

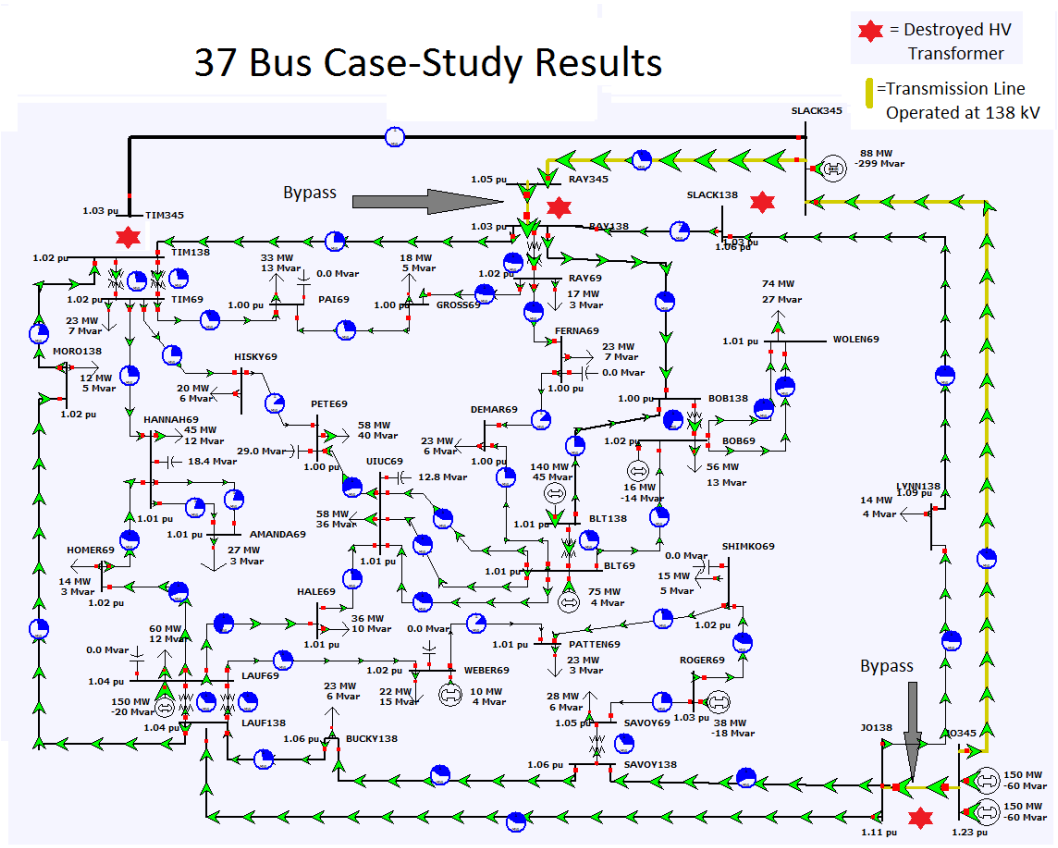

Figure 19. Post GMD 37 bus system with destroyed transformers

The arrows in Figure 19 represent the real power flowing through the system. It is important to notice that all six of the high voltage transformers have been removed from the system. Transmission lines have been installed to bypass

two of the critical transformers. The highlighted transmission lines have the equivalent impedance of comparable 138 kV lines. The power flow solution to the one-line diagram shows the system is fully operational and operating under the constraints of each component.

Bypassing the critical high voltage transformers in the power system after damage from a geomagnetic storm has occurred is more of a last resort solution. Utilities may be reluctant to spend hundreds of millions of dollars to protect their system from a 100-year storm. When the storm occurs, the damage to the transformers cannot be undone. Bypassing the damaged transformers with a patch transmission line is a viable solution to restoring power to the grid. Without bypassing the transformers, the outage could be more long-term since the inventory of high voltage transformers is too small and the time involved in installing the transformers is too large [4]. The point of this method is to restore power to as many of the customers as possible in a timely manner.

Utilities need to study the impact of GIC on their systems. This will give them information to make educated decisions on how to deal with the effects of high-impact low-frequency events on their systems. Like most engineering problems, there are tradeoffs involved, which should be studied and evaluated. Utilities should evaluate the risk of an event and plan appropriately. Being negligent to the idea of a HILF event having drastic effects on their systems is not a responsible answer.

CHAPTER 8

CONCLUSIONS

With the combined effort of modeling and simulation of power systems under the stress of a geomagnetic disturbance, future disasters can be mitigated by strategically protecting the critical/vulnerable points in power systems around the world from GIC. Once the models have been validated and incorporated into power analysis software, power system planning engineers can use tools to effectively reduce the impacts of GIC on their system. Mitigation strategies will be explored: transformer bypassing, installing of GIC blocking devices, power flow redistribution by intentional line outages, and load shedding schemes, to name a few. The importance of modeling the impacts of GIC on the low voltage system is still unknown and will be explored in the research. The most important parameters of the model still need to be identified. The short-term and long-term mitigation strategies of GIC need to be explored. From an operating perspective, operators must be ready to respond to a GMD event, given information of a storms arrival in a few hours to days timeframe. Long-term mitigation strategies become important when GIC blocking devices have been added to the system. GIC has the potential to be redistributed in the system since it can no longer enter/exit blocked points. How the GIC redistributes and how to appropriately plan for the redistribution is something that will be addressed with further

research. This allows for the development of a GIC “optimum power flow” algorithm. Topics of future research include: more detailed reactive power demand model of saturated transformers, effects of harmonics on power system components due to transformer saturation, a more in-depth look at modeling the interaction between the magnetosphere and the Sun, and the effects of GIC on lower voltage (sub 500 kV) networks, to name a few. This research has tremendous potential as the threat of a storm is imminent and the public becomes more aware of the dangers attributed to a GMD’s interaction with the power system.

REFERENCES

[1] T. R. Hutchins and T. J. Overbye, "The effect of geomagnetic disturbances on the electric grid and appropriate mitigation strategies," in *North American Power Symposium*, Boston, MA, 2011.

[2] S. Macmillan, (2004/Rev.2006), Earth's Magnetic Field, in *Geophysics and Geochemistry*, Ed. Jan Lastovicka, in *Encyclopedia of Life Support Systems (EOLSS)*, Developed under the Auspices of the UNESCO, Eolss Publishers, Oxford, UK.

[3] C. Balch. (2011, Dec.), "The K-index," National Oceanic and Atmospheric Administration, unpublished. [Online]. Available: http://www.swpc.noaa.gov/info/Kindex.html

[4] North American Electric Reliability Corporation and the United States Department of Energy, "High-Impact, Low-Frequency Event Risk to the North American Bulk Power System," Atlanta, GA, June, 2010.

[5] J. G. Kappenman, "A perfect storm of planetary proportions," *IEEE Spectrum*, vol. 49, pp. 26-31, February 2012.

[6] J. G. Kappenman, "Geomagnetic storms and their impacts on the U.S. power grid," Metatech Corporation, Goleta, CA, Meta-R-319, January 2010

[7] J. G. Kappenman and V. D. Albertson, "Bracing for the geomagnetic storms," *IEEE Spectrum*, vol. 27, pp. 27-33, March 1990.

[8] North American Electric Reliability Corporation and the United States Department of Energy, "Effects of geomagnetic disturbances on the bulk power system," Atlanta, GA, 2012.

[9] J. D. Glover, M. S. Sarma and T. J. Overbye, *Power System Analysis and Design*, Toronto: Thomson Learning, 2008.

[10] V. D. Albertson, J. G. Kappenman, N. Mohan and G. A. Sharbakka, "Load-flow studies in the presence of geomagnetically-induced currents," *IEEE Power Apparatus and Systems*, vol. PAS-100, pp. 594-607, 1981.

[11] J. S. Foster, E. Gjelde, R. J. Hermann, H. M. Kleupfel, R. L. Lawson, G. K. Soper, L. L. Wood and J. B. Woodard, "Report of the commission to assess the threat to the United States from electromagnetic pulse (EMP) attack," www.empcommission.org, 2008.

[12] National Academy of Sciences, "Severe space weather events-understanding societal and econmic impacts," National Research Council, Washington, D.C., Rep. 12507, 2008.

[13] V. D. Albertson and J. A. Van Baelen, "Electric and magnetic fields at Earth's surface due to auroal currents," *IEEE Transactions on Power Apparatus and Systems,* vol. PAS-89, pp. 578-584, 1970.

[14] D. H. Boteler and R. J. Pirjola, "The complex-image method for calculating the magnetic and electric fields produced at the surface of the Earth by the auroral electrojet," *Geophysica,* vol. 132, no. 1, pp. 31-40, 1997.

[15] D. H. Boteler and R. J. Pirjola, "Modelling geomagnetically induced currents produced by realistic and uniform electric fields," *IEEE Trasactions on Power Delivery,* vol. 13, no. 4, pp. 1303-1308, 1998.

[16] R. Horton, D. H. Boteler, T. Overbye, R. J. Pirjola, and R. Dugan, "A test case for the calculation of geomagnetically induced currents," submitted to *IEEE Transactions on Power Delivery*, March 2012.

[17] R. A. Walling and A. H. Khan, "Characteristic of transformer exciting-current during geomagnetic disturbances," *IEEE Transactions on Power Delivery*, vol. 6, no. 4, pp. 1707-1714, 1991.

[18] X. Dong, Y. Liu, and J. G. Kappenman, "Comparative analysis of exciting current harmonics and reactive power consumption from GIC saturated transformers," in *Proceedings of IEEE Power Engineering Society Winter Meeting,* vol. 1, pp. 318-322, 2001 .

[19] P. W. Sauer and M. A. Pai, *Power System Dynamics and Stability.* Champaign: Stipes Publishing, 1997.

[20] Emprimus, 2011, Emprimus Solidground Neutral DC Blocking System, http://emprimus.com/emp-iemi_products/grid-and-transformer-protection.php.

[21] T. R. Hutchins and T. J. Overbye, “Power flow studies in the presence of geomagnetically induced currents,” in *Proceedings of the Power and Energy Conference at Illinois*, Urbana, Illinois, 2012.